

UC San Diego

UC San Diego Previously Published Works

Title

Distributed Mode and Power Selection for Non-Orthogonal D2D Communications: A Stochastic Approach

Permalink

<https://escholarship.org/uc/item/4kw621gh>

Journal

IEEE Transactions on Cognitive Communications and Networking, 4(2)

ISSN

2372-2045

Authors

Librino, Federico

Quer, Giorgio

Publication Date

2018-06-01

DOI

10.1109/tccn.2018.2809721

Copyright Information

This work is made available under the terms of a Creative Commons Attribution-NonCommercial-NoDerivatives License, available at <https://creativecommons.org/licenses/by-nc-nd/4.0/>

Peer reviewed

# Distributed Mode and Power Selection for non-Orthogonal D2D Communications: a Stochastic Approach

Federico Librino, *Member, IEEE*, and Giorgio Quer, *Senior Member, IEEE*.

**Abstract**—The coexistence of device-to-device (D2D) and cellular communications in the same band is a promising solution to the dramatic increase of wireless networks traffic load, in particular in the presence of local traffic, when source and destination nodes are in close proximity. In this case, the mobile nodes can communicate in a semi-autonomous way (D2D mode), with minimal or no control by the base station (BS), but they may create a harmful interference to the cellular communications. In order to avoid it, we design a distributed approach that allows the mobile node to acquire in real time local information by observing few channel and topology parameters. Based on this information, each user can infer in advance not only the quality of its transmission, but also its impact on other ongoing surrounding communications towards the BS. This enables a smart, adaptive mode and power selection performed with a network wide perspective. Differently from most approaches, this selection is made autonomously by each D2D sources, with no need for a centralized scheduling. We compare our strategy to the state-of-the-art in the same distributed network scenario, showing the importance of exploiting local information for a dynamic, interference aware power and mode selection.

## I. INTRODUCTION

The recent advancements in cellular networks introduced faster and more reliable communications, both in the uplink and the downlink, due to a smarter assignment of time/frequency resources. In particular, LTE technology led to a huge increase in the overall network capacity thanks to innovations in coding/decoding devices and to the application of novel communication strategies.

The amount of traffic load is also increasing dramatically: social media have driven the spread of file sharing (photos, music, and videos), while many widespread mobile applications require frequent data exchanges with a remote server. Handling this amount of communications with a given quality of service (QoS) is challenging. Currently, 5G technologies are being developed to answer the need for further increasing network capacity, and among them, device-to-device (D2D) communications are attracting increasing attention [1]–[6]. In particular, D2D communications are a valid alternative in the presence of traffic to be exchanged locally, i.e., when source

and destination are in close proximity, as in file exchange between two collocated user equipments (UEs), in certain gaming applications, or when a UE downloads local information from wireless sensors in a smart city [7].

In this work, we divide the UEs based on their traffic, and we distinguish between UEs with global traffic (UE-GTs), and with local traffic (UE-LTs). A UE-GT is a cellular user communicating with the corresponding base station (BS), since its intended destination is not in close proximity. A UE-LT can instead transmit its packets directly to its corresponding destination, which is located within a short distance, in the same or in an adjacent network cell.

If an orthogonal channel is available, it is possible to allocate it to the D2D communication and to avoid any interference to the BS. The problem is more complex when the spectrum resources must be shared with the BS (non-orthogonal channel). In this case, we can distinguish two approaches. The first is a centralized approach, which consists in letting the BS schedule all the D2D communications and to balance the overall interference level [8], [9] by exploiting full channel state information (CSI) about all of the involved links. Centralized schemes based on global information can achieve the optimal performance, but this acquisition is not always possible since it requires a considerable overhead at the BS to collect CSI, and it may be significantly disadvantageous in the case of close proximity between the UE-LTs. The second approach includes distributed schemes relying only on local information, either static or dynamic. The knowledge of local information is exploited by each user to estimate the effect of the surrounding network environment on its performance, thus allowing to perform the mode, power and channel selection to attain a target QoS.

The drawback of this distributed approach is that it usually aims only at keeping the user performance close to a pre-defined level, but completely neglects the potentially strong impact that a transmission can cause on the surrounding communications.

In this work, we aim at incorporating also this aspect into a distributed power and mode selection scheme. To this end, we design a distributed strategy to deal with non-orthogonal D2D transmissions without a centralized coordination by the BS. The uplink resources of the cellular network are shared between the UE-GTs (transmitting to the BS), and the UE-LTs (the D2D terminals), while no additional spectrum resources are reserved for the D2D data communications. Our distributed approach is based solely on local information, including

F. Librino is with the Italian National Research Council, 56124 Pisa, Italy (e-mail: federico.librino@iit.cnr.it).

G. Quer is with the Scripps Research Institute, 3344 North Torrey Pines Court, La Jolla, CA 92037, and was with the University of California, San Diego, 9500 Gilman Dr., La Jolla, CA 92093 (e-mail: gquer@scripps.edu).

This work was partially supported by the Qualcomm Institute, University of California, San Diego, and by the Institute for Informatics and Telematics (IIT) of the Italian National Research Council.

critical time-varying parameters. However, differently from other schemes, this information is then exploited at each D2D source to estimate the impact of the selected transmission mode and power level on the neighboring nodes, in terms of capacity reduction. This allows us to find a tradeoff between a selfish mode/power selection, which aims exclusively at maximizing the user performance, regardless of the surrounding communications, and a network aware selection, which is determined solely by the network conditions and allows only non interfering D2D communications. Such tradeoff is enforced by a protection mechanism employed by the core network, thus granting a superior global network performance.

The main contributions of this paper are summarized in the following.

- We propose a novel transmission strategy for a UE aiming to transmit local traffic through D2D communications by sharing the uplink resources with the cellular network. The novelty of the approach resides in the fact that the scheduling is autonomously performed at the D2D node using local topological and channel information, not only to predict the D2D quality of service, but also its impact on the capacity of surrounding channels.
- A Bayesian Network (BN) probabilistic approach is proposed in our scenario to cope with the limited and unreliable information collected locally, in order for the UE to choose the D2D mode only if the network conditions are suitable. We stress the fact that in our scenario it is not possible to seek for a global optimal solution, since the available information is limited.
- We showcase the advantages of our stochastic technique, as compared to the state-of-the-art, in the distributed scenario considered. The performance is evaluated at the link level to understand the behavior of the UE-GTs and the UE-LTs. Then the system level performance is evaluated, showing a substantial gain of our strategy for the UE-GTs with respect to other state-of-the-art techniques. These results confirm that, in the absence of a centralized controller, using local information to predict both the expected quality of communication and the impairment caused to the surrounding nodes can significantly improve the network performance.

The rest of the paper is organized as follows. We overview the most recent 3GPP releases in D2D communications and the related works in Sec. II. In Sec. III we describe our distributed network scenario and the corresponding system model, while our proposed technique is outlined in Sec. IV. The details of the BN probabilistic approach are illustrated in Sec. V, then the results for the direct D2D transmissions are shown in Sec. VI. Sec. VII concludes the paper.

## II. RELATED WORK

The concept of D2D proximity services in an LTE network has been proposed by 3GPP as a promising way to either reduce the traffic load at the BSs, or to extend service beyond cellular coverage in emergency scenarios, where the core network may be unavailable [1], [3]. Most of the opportunities and challenges foreseen by 3GPP in establishing D2D connections in a cellular network, including peer discovery, resource

allocation, synchronization and interference management, are discussed in [2]. Pricing models for D2D are introduced in [4], while multiple-input-multiple-output (MIMO) D2D communications are discussed in [5], and an opportunistic multi-hop forwarding technique is presented in [10]. In these papers, D2D communications are investigated as a mean to extend the cellular coverage, i.e., a mobile terminal may forward the data packets to/from another terminal that is not in the range of a BS. Differently from these works, in our paper we do not exploit D2D to extend the coverage area of the BS, but to allow a direct communication among UEs in close proximity.

The use of an orthogonal channel for D2D communications is investigated in [11], where nodes in a single cell scenario are organized into clusters by centralized scheduling. In our work, conversely, we focus on non-orthogonal spectrum sharing between nodes transmitting to the BS, and nodes in D2D mode. In this case, there are two ways in the state-of-the-art to access the spectrum. 1) The D2D source can transmit only on a temporarily free channel (overlay), without interfering with the BS, and 2) it can also use a busy channel by limiting the resulting interference (underlay). In [12] both options are analyzed in terms of coverage probability and connectivity of the D2D network, by means of stochastic geometry tools.

In the literature, the resource allocation in an underlay approach in a multicell scenario is often done by a centralized entity (usually located at the BS) based on the available and collected information about the channels [13]–[15]. An optimal allocation of D2D and cellular (D2B) communications, following the underlay principle, is detailed in [13], where mutual interference constraints are taken into account to derive a centralized scheduling. CSI is also exploited in [15]; here, the idea is to limit the interference of D2D communications over cellular links by deriving an outage constrained precoding at the D2D source. Also in this case, where multiple antennas are considered, a proper centralized optimization problem is set up, taking into account that only partial CSI is available on some channels. An optimal centralized transmission strategy based on a Markov decision process is instead derived in [16] in a single-cell scenario. In the multi-cell scenario, however, this global optimization would result in a computationally unfeasible state space cardinality.

A main difference between our approach and the aforementioned works lies in our strategy to mitigate the interference, which is not based on a centralized optimization problem (assuming full or partial CSI over all the channels), as in [9], [11], [13], [17]. Instead, we rely only on local information, distributedly acquired thanks to the observation of topology and channel parameters, and on its exploitation via a BN approach.

An interesting solution in a similar scenario, without a centralized coordination entity, is proposed in [18]. In that work, D2D communications with power control can be performed using uplink resources only if source and destination are within a maximum distance, as in our approach, in order to keep interference within an acceptable level. Nonetheless, the choice to transmit directly to the receiving UE or to the BS is based only on parameterized topological considerations, thus lacking the fundamental adaptiveness of our approach. This

approach is summarized in Sec. IV-E, and its performance is compared to our work in Sec. VI.

Another distributed approach, the Distributed Power and Mode Selection (DPMS), is presented in [19], where each potential D2D transmitter can autonomously perform mode and power selection based on the measured interference levels at both the intended D2D receiver and at the BS. This scheme shows an increased adaptivity, but local information is used only to estimate the D2D transmission quality, thus ignoring the potentially high interference caused to the surrounding BS. We highlight the importance of this aspect by comparing our technique with DPMS in Sec. VI.

Other distributed approaches are instead implemented in multi-channel scenarios [20]–[22], thus including also resource allocation. In [20], users are distributedly partitioned into coalitions, and power control algorithms are implemented to maximize the sum-rate within each coalition. Here, however, each user has its own dedicated uplink resources, which can be shared among multiple users in such a way that the interference on shared channels is minimized. Coalitions are created also in [21], each one composed by the users which selected the same transmission mode. Each coalition aims at minimizing the overall transmit power while attaining a predefined target rate. However, the analysis is limited to a single cell scenario. Authors in [22] propose a distributed channel and power selection for D2D sources based on a Stackelberg game with pricing. This is also a stochastic approach, since the D2D transmitters adopt a stochastic learning algorithm to minimize interference. However, mode selection is not considered, downlink resources are exploited, and a single cell scenario is studied.

Finally, in our previous works, we applied a probabilistic approach to the design of a network-aware retransmission strategy [23] in an ad hoc wireless network, and to promote cooperation between two adversarial ad hoc networks that share the same spectrum [24]. In [25], we investigated a two-tier network, where the D2D tier coexists with the D2B tier thanks to a probabilistic approach. In that work, in order to make the inference on the amount of interference to the BS, the potential D2D source needed to collect information about all the channels to all its neighbors, including the neighboring BSs and D2D nodes, thus making this approach unfeasible. Furthermore, the potential D2D source in that work did not have the choice to adaptively switch to a D2B mode, as in the current work, and power control was not adopted.

### III. SYSTEM MODEL

#### A. Primary tier: cellular users

In this paper, we study a 4G cellular network, where BSs are distributed according to a bi-dimensional Poisson point process  $\Psi_V$  with intensity  $\lambda_V$ . In our scenario,  $\mathcal{B}$  is the set of BSs, which partition the plane into Voronoi cells  $v \in \{1, \dots, V\}$ , and  $B^{(v)} \in \mathcal{B}$  is the BS located in cell  $v$ . Time is slotted, and divided into *epochs*, each one composed by  $N_e$  consecutive time slots.

We focus on the uplink, and full frequency reuse is assumed. We consider a fully loaded network where in each cell  $v$  there

are  $N_c$  uplink channels, and there is a non-empty set  $\mathcal{W}^{(v)}$  of users, randomly deployed within the cell. In our model, all the sources are backlogged, hence all the users in  $\mathcal{W}^{(v)}$  always have data packets to transmit, and we set  $|\mathcal{W}^{(v)}| \geq N_c$ . Intra-cell interference is not allowed in the primary tier, hence in cell  $v$ , at the beginning of each epoch, each uplink channel  $c$  is assigned to one of the users in  $\mathcal{W}^{(v)}$ , which transmits for the entire epoch, thus the maximum number of active users is  $N_c$ . Since all the channels have the same statistics, in the following we can limit our analysis to a single uplink channel. The same analysis holds for the remaining channels, under the assumption that channel selection has been already performed by each user.

In general, a different user in  $\mathcal{W}^{(v)}$  can be granted access to the considered channel at each epoch, following a centralized scheduling procedure. Since we do not deal with the users scheduling, in this paper we assume that only the same UE-GT  $U^{(v)} \in \mathcal{W}^{(v)}$  can be allowed to transmit over channel  $c$  in every epoch. Nonetheless, our scheme can be extended to a more general scenario, and integrated with any kind of scheduling and channel selection procedure. A joint mode/power/channel selection may result in a better resource utilization, and is left as a promising direction for future work.

We define the set of all the cellular users in the network as  $\mathcal{U}_g = \cup_v \mathcal{W}^{(v)}$ . The users of this set are also called UE-GTs in the following. User  $U^{(v)}$  sets its transmit power to  $P_{U^{(v)}} = \rho d(U^{(v)}, B^{(v)})^\alpha$ , where  $\rho$  is a predefined target received power level,  $d(X, Y)$  indicates the Euclidean distance between terminals  $X$  and  $Y$  and  $\alpha$  is the path loss exponent. In order to avoid truncation outage effects, we randomly deploy  $U^{(v)}$  within cell  $v$  under the condition  $d(U^{(v)}, B^{(v)}) \leq d_R$ , where  $d_R = (P_M/\rho)^{1/\alpha}$  and  $P_M$  is the maximum allowed transmit power.

A threshold model is assumed for decoding: a data packet sent at time slot  $k$  is correctly decoded if the SINR at the destination is greater than a fixed decoding threshold,  $\phi$ . All channels are modeled as Rayleigh channels, so the SINR at  $B^{(v)}$  for the signal from  $U^{(v)}$  at time slot  $k$  can be written as

$$\begin{aligned} \Gamma_{B^{(v)}}(k) &= \frac{P_{U^{(v)}} |h(B^{(v)}, U^{(v)}, k)|^2}{(N_0 + I_{B^{(v)}}(k)) d(U^{(v)}, B^{(v)})^\alpha} \\ &= \frac{\rho |h(B^{(v)}, U^{(v)}, k)|^2}{N_0 + I_{B^{(v)}}(k)}, \end{aligned} \quad (1)$$

where  $N_0$  is the noise power, and  $h(X, Y, k)$  is the fading coefficient between terminals  $X$  and  $Y$  at time slot  $k$ , which is symmetric and independent from the channel gain between other pairs of nodes. It is modeled as

$$h(X, Y, k) = \varrho h(X, Y, k-1) + \sqrt{1 - \varrho^2} \zeta, \quad (2)$$

where  $\zeta$  is an independent Gaussian random variable with zero mean and unit variance, and  $\varrho$  is the correlation coefficient [26].

$I_{B^{(v)}}(k)$  is the interference level at the BS, introduced in

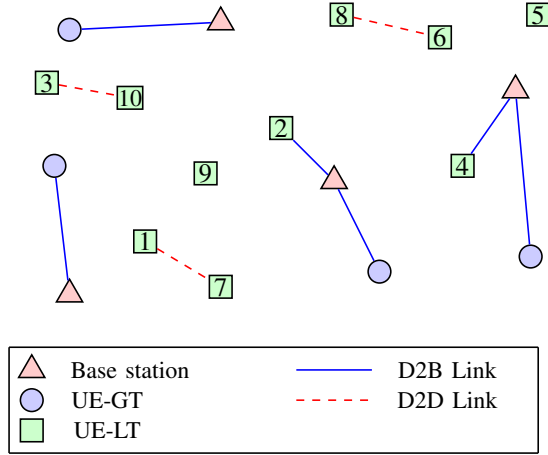


Fig. 1. Considered multi-cell scenario. UE-LTs may transmit directly to their associated BS (UE-LTs 2 and 4), or they can communicate with each other in a D2D fashion (e.g., UE-LTs 3 and 10).

(1), which is defined as

$$I_{B^{(v)}}(k) = \sum_{w \neq v} P_{U^{(w)}} \frac{|h(U^{(w)}, B^{(v)}, k)|^2}{d(U^{(w)}, B^{(v)})^\alpha} + \sum_{U_S \in \mathcal{U}_\ell} P_{U_S} \frac{|h(U_S, B^{(v)}, k)|^2}{d(U_S, B^{(v)})^\alpha}, \quad (3)$$

where the two terms account for the transmissions on channel  $c$  from users in other cells and from other D2D sources (in the set  $\mathcal{U}_\ell$ , as detailed in the next section), respectively.

#### B. Secondary tier: UEs with local traffic (UE-LTs)

In our network scenario, besides the cellular users ( $\mathcal{U}_g$ ), we consider an additional set of users ( $\mathcal{U}_\ell$ ), which are sources of *local traffic*, namely UE-LTs. Each UE-LT has data to transmit to another user located in its proximity. The UE-LTs are distributed according to a bi-dimensional Poisson process  $\Psi_D$  with intensity  $\lambda_D$ , independent from  $\Psi_V$ . Each UE  $U_S \in \mathcal{U}_\ell$  is associated to a receiver uniformly deployed within a circle centered at the location of  $U_S$  and with radius  $d_L$ .

Differently from the cellular users in  $\mathcal{U}_g$ , the UE-LTs are not required to transmit to the corresponding BS. In fact, given the small distance from their intended receiver, it may be convenient for a UE-LT to set up a D2D communication. We consider non-orthogonal D2D transmissions, which take place on the considered uplink channel<sup>1</sup>. A UE-LTs  $U_S \in \mathcal{U}_\ell$  in cell  $v$  can hence choose between two transmission modes.

**D2D mode.** The data packet is sent directly to the corresponding receiver  $U_D$  by reusing the same uplink channel as the cellular user  $U^{(v)}$ . The transmission power  $P_S$  can be chosen within a set  $\Pi$  of logarithmically spaced levels, and the transmission succeeds if the SINR at  $U_D$  is greater than  $\phi$ , that is, if

$$\Gamma_{U_D}(k) = \frac{P_S h|U_S, U_D, k|^2}{(N_0 + I_{U_D}(k)) d(U_S, U_D)^\alpha} \geq \phi, \quad (4)$$

<sup>1</sup>We assume that the uplink channel selection has already been performed. The UEs in  $\mathcal{U}_\ell$  are those that selected the considered uplink channel  $c$ . Analogous sets of UE-LTs can be identified for the other uplink channels.

where  $I_{U_D}(k)$  is the interference perceived at  $U_D$ , and has an expression analogous to (3). This transmission can start at any time slot within an epoch, and proceeds until the end of the epoch.

**D2B mode.** The data packet is first transmitted to the BS, which subsequently forwards it to  $U_D$  on a downlink channel. If it selects this mode,  $U_S$  must first issue a resource allocation request to the BS  $B^{(v)}$ , which will grant  $U_S$  the exclusive access to the channel in one of the subsequent epochs (thus halting the transmission from  $U^{(v)}$ ). The selected transmit power level  $\pi \in \Pi$  in this case is the minimum one greater than  $\rho d(U_S, B^{(v)})^\alpha$ . Notice that, although the D2B mode allows  $U_S$  to avoid mutual interference with  $U^{(v)}$ , it also implies that the uplink channel is to be orthogonally shared with  $U^{(v)}$  (and possibly with other UE-LTs in the same cell, also selecting the D2B mode), thus increasing the data delivery delay.

## IV. DISTRIBUTED MODE AND POWER SELECTION

### A. Problem Formulation

At the beginning of each epoch, each D2D source in  $\mathcal{U}_\ell$  can decide whether to issue a request for channel access to the BS (D2B mode) or to select the D2D mode. In the latter case, the transmission power must also be chosen by the D2D source within the set  $\Pi$ . The optimal mode/power selection depends on the metric to be optimized. In this paper, we are interested in the spectral efficiency, since it can offer a global view of the spectrum utilization throughout the network. The instantaneous spectral efficiency of a transmission from user  $i \in \mathcal{U}_g \cup \mathcal{U}_\ell$  at time slot  $k$  is given by:

$$\mathcal{R}_i(k) = \theta \ln(1 + \Gamma_i(k)), \quad (5)$$

where  $\Gamma_i(k)$  is the SINR at the intended receiver of the transmission from UE  $i$ , while  $\theta$  is equal to 1 if the transmission is a D2D communication, and is equal to 1/2 if instead  $i$  is transmitting to a BS. The presence of this factor is due to the fact that, if a D2B transmission is being performed, the data packet requires a second downlink transmission (not modeled in this paper) in order to be delivered to its destination, and the spectral efficiency must be halved.

The global spectral efficiency is the sum of the spectral efficiency of all the users averaged over an entire epoch. The maximization of this metric is quite involved. Consider the indicator variable  $\chi_i$ , equal to 1 if UE  $i \in \mathcal{U}_g \cup \mathcal{U}_\ell$  is scheduled to transmit to the BS of its own cell, which we call  $B(i)$ , and 0 otherwise. In several works, a centralized solution is proposed, based on an optimization problem which, in our scenario, can be formulated as

$$\max_{\mathbf{x}, \mathbf{P}} \frac{1}{N_e} \sum_{k=1}^{N_e} \left( \sum_{i \in \mathcal{U}_g} \mathcal{R}_i(k) + \sum_{j \in \mathcal{U}_\ell} \mathcal{R}_j(k) \right) \quad (6a)$$

$$\text{s.t. } \chi_i \in \{0, 1\}, \quad \forall i \in \mathcal{U}_g \cup \mathcal{U}_\ell \quad (6b)$$

$$\chi_i + \sum_{j \in \mathcal{U}_\ell(B(i))} \chi_j = 1, \quad \forall i \in \mathcal{U}_g \quad (6c)$$

$$P_j \in \Pi \cup \{0\}, \quad \forall j \in \mathcal{U}_\ell : \chi_j = 0, \quad (6d)$$

where  $\mathcal{U}_\ell(B) \subset \mathcal{U}_\ell$  is the subset of UE-LTs located in the cell of BS  $B$ , while the spectral efficiency in (5) can be rewritten as

$$\mathcal{R}_i(k) = \frac{1}{2} \ln(1 + \chi_i \Gamma_{B(i)}(k)), \quad (7)$$

for  $i \in \mathcal{U}_g$ , and as

$$\mathcal{R}_j(k) = \frac{1}{2} \ln(1 + \chi_j \Gamma_{B(j)}(k)) + \ln(1 + (1 - \chi_j) \Gamma_{D(j)}(k)), \quad (8)$$

for  $j \in \mathcal{U}_\ell$ . Here,  $D(j)$  is the receiver associated with the UE-LT  $j$ . Notice that  $\chi_i = 0$ , for  $i \in \mathcal{U}_g$ , implies that UE  $i$  does not transmit in the considered epoch, while  $\chi_j = 0$ , for  $j \in \mathcal{U}_\ell$ , implies that  $j$  either does not transmit at all, or it transmits via D2D to its associated receiver, depending on the selected value for  $P_j$ , which can be equal to 0 or belong to  $\Pi$ . The maximization is done over the vector  $\mathbf{X}$ , containing all the indicator variables, and over the vector  $\mathbf{P}$ , containing all the transmit power levels for the UE-LTs in D2D mode:

$$\mathbf{X} = \{\chi_i, i \in \mathcal{U}_g \cup \mathcal{U}_\ell\}, \quad \mathbf{P} = \{P_j, j \in \mathcal{U}_\ell : \chi_j = 0\}. \quad (9)$$

In (6a), we consider that all the transmissions must start at the beginning of the epoch, and that the transmit power used for a D2D communication is fixed during the entire epoch. Even with these constraints, the solution of the maximization problem is quite involved: for a single cell,  $(|\Pi|+1)^{N_s-1}(|\Pi|+N_s+1)$  allocations are possible, where  $N_s$  is the number of UE-LTs in the cell. In addition, given the expressions of the SINRs, the fading coefficients of all the channels for all the time slots must be known in order to find the best allocation. A global optimization, taking into account also the inter-cell interference, is therefore clearly unfeasible for  $N_s \gg 1$ .

### B. Distributed Solution

Instead of relying on a global, centralized optimization, in this paper we opt for a suboptimal distributed mode/power selection, without the need for a centralized entity. Each UE autonomously decides whether to issue a resource request to the BS (for D2B transmission in a subsequent epoch) or to start a D2D communication, and it selects the transmit power. This scalable approach strongly alleviates the burden required to the core network. On the flip side, however, the lack of a global coordination requires a careful mode selection, in order to limit the intra-cell and inter-cell interference.

Since we are interested in a distributed mode/power selection, we need to shift from a global metric to a local one. In our distributed approach, in fact, each UE-LT  $U_S \in \mathcal{U}_\ell$  aims at increasing its own expected spectral efficiency towards a target value, using only partial knowledge about local topology and surrounding nodes. The details of this approach will be described in Sec. IV-D.

The main assumptions in our scenario are listed in the following.

- An out-of-band channel, namely  $c_0$ , is available for the UE-LTs. This channel is used to send feedback or to exchange short control packets for setting up the D2D communication.

- Each UE-LT  $U_S$  is aware of the local topology<sup>2</sup>. In this study, the local topology includes the locations of  $U_S$  itself, of its intended destination and of the BS  $B^{(v)}$  located in the same cell  $v$ .

- $U_S$  can acquire information about the condition of its channel towards the BS  $B^{(v)}$  and about the current SINR  $\Gamma_{B^{(v)}}$  perceived at the BS  $B^{(v)}$  (e.g., by overhearing a proper downlink control channel).

- A BS constantly monitors the signal received on channel  $c$ , and is able to recognize the presence of D2D communications within its cell.

A distributed mode and power selection, aiming at maximizing only the transmitter's performance, can easily lead to selfish behaviors. This in turn may cause a D2D communication to strongly interfere with other D2D communications and with the transmissions of cellular users, thus lowering the overall network performance. Notice that the interference to D2B communications is more relevant, since D2B transmitters are the legitimate users of the uplink channel, and their communications must be protected to guarantee a target QoS. In order to tackle this issue, we adopt the two following refinements.

**R1)** D2D communications are preceded by a short RTS/CTS exchange on the out-of-band channel  $c_0$ . This allows the D2D transmitter  $U_S$  to inform surrounding UE-LTs of an incoming transmission. Furthermore, in the CTS, the intended receiver  $U_D$  can inform  $U_S$  of the channel quality and of the current perceived interference level.

**R2)** We assume that a *protection mechanism* is adopted by the cellular network to protect the D2B communications. At each time slot  $k$ , from the SINR  $\Gamma_{B^{(v)}}(k)$ , the BS can compute the instantaneous capacity  $C_{B^{(v)}}(k) = \log(1 + \Gamma_{B^{(v)}}(k))$ . An ongoing D2D communication has a detrimental effect on the capacity, since it lowers the SINR. We define a novel metric, called *relative capacity loss*, at time slot  $k$  due to the D2D communication performed by  $U_S$  as

$$\Lambda(U_S, B^{(v)}, k) = 1 - \frac{C_{B^{(v)}}(k)}{C_{B^{(v)}}^{(-U_S)}(k)}, \quad (10)$$

where  $C_{B^{(v)}}^{(-U_S)}(k) = \log(1 + \Gamma_{B^{(v)}}^{(-U_S)}(k))$  is the estimated capacity which would have been achieved if  $U_S$  had not transmitted. The modified SINR is hence equal to

$$\Gamma_{B^{(v)}}^{(-U_S)}(k) = \frac{\rho |h(B^{(v)}, U^{(v)}, k)|^2}{N_0 + (I_{B^{(v)}}(k) - P_{sb})}, \quad (11)$$

where  $P_{sb} = P_S d(U_S, B^{(v)})^{-\alpha} |h(U_S, B^{(v)}, k)|^2$  is the power received at the BS from  $U_S$ . Whenever a capacity loss greater than a threshold  $\Lambda_M$  occurs, the BS broadcasts a warning message on the downlink channel, forcing  $U_S$  to stop its D2D transmissions until the end of the current epoch. We choose to utilize the relative capacity loss, instead of the interference or the SINR, since it allows to take into account also the useful signal strength and to identify the interference contribution of the various D2D sources. Henceforth, it better captures the detrimental effect of the D2D transmission from  $U_S$ . The

<sup>2</sup>The performance increases if topology information about other nodes is also available, but at the price of a higher overhead necessary to acquire it.

capacity loss limit  $\Lambda_M$  is a system parameter that can be tuned to balance the tradeoff between offloading the transmissions over D2D links and suffering an increased interference level.

In the next sections, we will detail how these countermeasures can be incorporated in an effective distributed mode/power selection strategy.

### C. Interference Estimation

The presence of the protection mechanism poses a severe limitation to the allowed transmission power for a UE-LT in D2D mode. In fact, while a low power can lead to a reduced spectral efficiency during the epoch, an excessively high one, triggering the protection mechanism, would lead to a transmission stop, and hence to a zero efficiency. Differently from the interference perceived at the D2D receiver, which can be conveyed to the transmitter during the handshaking, a feedback from the BS is unlikely to be admissible, since it would require a consistent amount of overhead.

It is therefore pivotal to use the available information to estimate the capacity loss which would be caused at the BS by a D2D transmission, and properly set the transmit power level. According to the assumptions listed in the previous section, a UE-LT in cell  $v$  has local topology information, and can collect, at time slot  $k$ , information about its channel towards the BS  $B^{(v)}$ . Let us call  $\mathcal{P}_C(U_S, k)$  the set of useful information available at  $U_S$  at time slot  $k$ , defined as

$$\mathcal{P}_C(U_S, k) = \left\{ d(U_S, B^{(v)}), h(U_S, B^{(v)}, k), \Gamma_{B^{(v)}}(k) \right\}, \quad (12)$$

where  $d(U_S, B^{(v)})$  can be considered fixed over short time periods. Estimating the expected capacity loss at BS  $B^{(v)}$  caused by a D2D transmission from  $U_S$  is not straightforward: channel fading coefficients are not fixed, although temporally correlated, and new D2D communications, in the same or adjacent cells, may start in the subsequent time slots, thus leading to unpredictable capacity variations at the BS.

Our proposed solution is to estimate the distribution of the capacity loss at the BS, for any possible transmit power level  $\pi \in \Pi$ , using the parameters in  $\mathcal{P}_C(U_S, k)$ . A mathematical derivation of this distribution is quite involved, since it also depends on the mode and power selection of other UE-LTs in the same and in adjacent cells, which is not known at  $U_S$  a priori. We therefore rely on a properly designed Bayesian network  $\text{BN}_{\text{int}}$ , which estimates the distribution of the capacity loss in the subsequent slot  $k+1$  using, as input, the parameters in  $\mathcal{P}_C(U_S, k)$  and a transmit power level  $\pi \in \Pi$ . The details on the BN approach adopted and its complexity are illustrated in Sec. V.

The cumulative distribution function (CDF) of the capacity loss can be written as

$$\begin{aligned} & F_{\Lambda(U_S, B^{(v)}, k+1)}(x|\pi, \mathcal{P}_C(U_S, k)) \\ &= P \left[ \Lambda(U_S, B^{(v)}, k+1) \leq x|\pi, \mathcal{P}_C(U_S, k) \right]. \end{aligned} \quad (13)$$

Using this distribution, we can calculate the probability  $p_{\text{blo}}(\pi)$  of triggering a blockage for the given transmit power level  $\pi$ , i.e.,

$$p_{\text{blo}}(\pi) = 1 - F_{\Lambda(U_S, B^{(v)}, k+1)}(\Lambda_M|\pi, \mathcal{P}_C(U_S, k)). \quad (14)$$

The blockage probability  $p_{\text{blo}}(\pi)$  quantifies the cost of selecting a transmit power level  $\pi$ , and hence makes it possible to find a tradeoff between a high D2D transmission quality towards  $U_D$ , and a low interference level caused at the BS.

Notice that we can potentially add any kind of available information as an input for the BN, since we rely on a stochastic tool for the interference estimation, rather than on mathematical expressions. The available information may include also upper layer quantities, like buffer occupancy, running applications types, traffic statistics, or buildings and walls location. We leave this improvement as an interesting direction for future work.

### D. Aware strategy, AWA-S

We propose a network aware strategy, which we name AWA-S. It is a transmission strategy relying on local information to select transmission mode and power based on the BN approach. This strategy works as follows. At the beginning of each epoch, a UE-LT not scheduled for transmission towards the BS, namely  $U_S$ , randomly selects a time slot  $k$ , with  $2 \leq k \leq N_w + 1$ , to attempt its D2D transmission. The quantity  $N_w < N_e$  defines a contention window, which is meant to spread the starting slot of different D2D sources over time.

At time slot  $k-1$ ,  $U_S$  sends the short RTS on the out-of-band channel  $c_0$ . The intended destination  $U_D$  replies with a CTS, where it reports the current value of the channel fading  $|h(U_S, U_D, k-1)|^2$ , as well as its current perceived interference value  $I_{U_D}(k-1)$ . Notice that this value includes the interference from other surrounding D2D communications which selected an earlier slot to start transmission. Subsequently,  $U_S$  performs the following four steps.

**S1)** At time slot  $k-1$ , it collects the parameters in  $\mathcal{P}_C(U_S, k-1)$ .

**S2)** It repeatedly exploits  $\text{BN}_{\text{int}}$  to estimate the distribution of  $\Lambda(U_S, B^{(v)}, k)$  for any possible value  $\pi \in \Pi$  of the transmit power. From these distributions, the conditional cumulative distribution function  $F_{\Lambda(U_S, B^{(v)}, k)}(x|\pi, \mathcal{P}_C(U_S, k-1))$  of the capacity loss is derived, and the blockage probability is computed for any power level according to (14).

**S3)** It determines the maximum transmit power level  $\pi_s \in \Pi$  which satisfies

$$p_{\text{blo}}(\pi_s) \leq \xi, \quad (15)$$

and the minimum transmit power  $\pi_m \in \Pi$  which satisfies

$$\frac{\pi_m |h(U_S, U_D, k-1)|^2 d(U_S, U_D)^{-\alpha}}{N_0 + I_{U_D}(k-1)} \geq \phi. \quad (16)$$

In (15),  $\xi$  is a tunable parameter, which we call *residual blockage probability*. Low values of  $\xi$  translate into a conservative strategy, while higher transmission powers are chosen as  $\xi$  increases. Notice that  $\pi_m$  is the minimum transmit power required to have a SINR greater than the decoding threshold  $\phi$ , while  $\pi_s$  is the maximum transmit power allowed in order to keep the blockage probability below  $\xi$ .

**S4)** If  $\pi_m \leq \pi_s$ , then a D2D transmission is possible.  $U_S$  starts a D2D transmission towards  $U_D$  at time slot  $k$  with power  $\pi_m$ ; the D2D communication will continue, with the same transmit power level, until the end of the current epoch.

If no value in  $\Pi$  could match condition (15), or if  $\pi_m > \pi_s$  then no D2D transmission is viable. In this case,  $U_S$  switches to D2B mode, and issues a request to the BS  $B^{(v)}$  to have the uplink channel assigned in the next epoch. Then, at the beginning of the next epoch,  $B^{(v)}$  assigns the channel to either  $U^{(v)}$ , or to one of the UE-LTs in cell  $v$  which issued a resource request. We do not focus on a specific scheduling in this work, hence we assume that this choice is made at random, but any scheme can be integrated. The UE-LTs whose request is not accepted start again the mode and power selection procedure in the subsequent epoch.

The strategy AWA-S can be opportunistically tuned by adapting the parameters  $\Lambda_M$  and  $\xi$ , choosing to favor either the UE-GTs or the UE-LTs. It is also worth noticing that while  $\Lambda_M$  can be seen as a predefined network parameter, the value of the residual loss probability  $\xi$  might be in principle selected independently by each UE-LT, in order to find a tradeoff between transmitting at higher power (high  $\xi$ ) and being silenced less frequently (low  $\xi$ ). A more conservative approach includes also the estimation of the capacity losses caused at other surrounding BSs. This option is not investigated in this paper since it would require a consistently higher overhead in order to collect all the necessary input parameters for the BN. Moreover, due to the exponential path loss model adopted in this work, the interference caused at the associated BS is the strongest one, and limiting this one is likely to strongly reduce the impairment to the rest of the network as well.

In order to test the effectiveness of exploiting local information in a distributed scheme, we compare AWA-S with two representative state-of-the-art mode/power selection strategies. The former, based only on topology information, has been proposed in [18], and we rename it as GEO-S. The latter instead takes advantage also of instantaneous channel information, thus adding a considerable degree of adaptivity. It has been described in [19], and is called DPMS in the following. GEO-S and DPMS offer a good reference point to evaluate the benefit attained by stochastically leveraging local information to infer transmission quality and interference impact. The observed performance gaps become good indicators to quantify the potential benefits offered by a distributed and dynamic exploitation of the available topology and channel information.

### E. Geographical strategy, GEO-S

GEO-S [18] is completely determined by topological information and by the value of the *bias factor*  $T_d$ . The topological information is composed by  $d(U_S, U_D)$ , the distance from  $U_S$  to its corresponding destination  $U_D$ , and  $d(U_S, B^{(v)})$ , the distance from  $U_S$  to its associate BS  $B^{(v)}$ . A direct D2D transmission will be performed only if

$$T_d d(U_S, U_D)^{-\alpha} \geq d(U_S, B^{(v)})^{-\alpha}, \quad (17)$$

so, when  $T_d = 0$ , no D2D communications are possible, whereas when  $T_d \rightarrow +\infty$  all the D2D potential sources are forced to select D2D mode. Since we are dealing with fixed topologies, the choice is made only once at the beginning of the transmissions, and is never changed. As to the transmission power, it is set according to the truncated channel

BN <sub>int</sub>	$X_1$	$\pi(U)$
	$X_2$	$ h(U, B, k) ^2 d(U, B)^{-\alpha}$
	$X_3$	$\Gamma_B(k)$
	$Y$	$\Lambda(U, B, k+1)$

TABLE I  
INPUTS AND OUTPUT FOR BN<sub>INT</sub>.

inversion rule. Recalling that  $\rho$  is the target power at the receiver, if D2D mode is chosen, the transmit power is set to  $P_t = \rho d(U_S, U_D)^\alpha$ , otherwise it is  $P_t = \rho d(U_S, B^{(v)})^\alpha$ .

The sources of local traffic in the same cell  $v$  that choose to transmit in D2B mode share the uplink channel  $c$  with the cellular UE  $U^{(v)}$  transmitting to the BS  $B^{(v)}$ . Time division is applied in this case, with all the involved UEs transmitting in a round robin fashion to avoid intra-cell interference and maintain fairness.

### F. Distributed Power and Mode Selection (DPMS)

The DPMS strategy was introduced in [19], and is a distributed power and mode selection strategy. Each UE-LT, at the beginning of each epoch, collects the SINR at the intended receiver and the one at the reference BS. It chooses D2D mode if the former is higher, and D2B mode otherwise, provided that another UE-LT has not already occupied the channel towards the BS. The transmission power is selected as the minimum necessary to reach the target SINR. This approach can be applied to transmit over multiple uplink channels, as done in [19].

Notice that, although this approach leverages some information about the channels of interest (towards the D2D receiver and the BS), it does not take into account the interference created at the BS when the D2D mode is selected, thus potentially impairing neighboring D2B communications.

## V. BAYESIAN NETWORKS

In this section, we detail the technique to learn the BNs of interest. A BN is a probabilistic graphical model [27], [28] used to describe the conditional dependence relations among a set of random variables. Each variable is represented as a node in the BN. The conditional dependences are represented in a directed acyclic graph (DAG), which defines the structure of the joint probability among all the nodes, and in particular it highlights the conditional independences among the nodes. This structure can be learned through an algorithm of structure learning, or it is given a priori based on previous knowledge of the data.

### A. BN for AWA-S strategy

The AWA-S strategy exploits a BN, whose inputs and outputs are listed in Table I.

BN<sub>int</sub> is used to determine how much a given transmission is harmful to the cell where it takes place. It estimates the capacity loss  $\Lambda(U, B, k)$  at the BS  $B$  due to the transmission by the user  $U$ . As output it provides the distribution of  $\Lambda(U, B, k+1)$ , from which the CDF  $F_{\Lambda(U, B, k+1)}(x)$  is calculated. This CDF is used to verify the condition in (15).



## B. BN learning

In this work, we considered the case in which the structure of the BN is given in the form of a naive BN. We have a set of  $N + 1$  random variables at each time  $t$ , i.e.,  $Y^{(t)}, X_1^{(t)}, \dots, X_N^{(t)}$ . Each variable is distributed according to a multinomial, i.e.,  $X_i^{(t)}$  has values in  $\{x_i(1), x_i(2), \dots, x_i(n_i)\}$  for all  $t$ , where  $n_i$  is the number of possible values assumed by  $X_i^{(t)}$ . If we consider the set of variables  $X_i^{(t)}$  for  $t \in \{1, 2, \dots, T\}$  we obtain the discrete time random process  $X_i$ , corresponding to a node in the DAG.

In a naive BN, there is only one parent node,  $Y$ , and  $N$  children nodes,  $X_1, \dots, X_N$ . In the corresponding DAG, there is an arrow (describing a conditional dependence) from  $Y$  towards each of the other nodes. A joint observation of all the nodes at instant  $t$  is the measurement of all their values at this instant. Let us assume that 1) we have a dataset  $\mathcal{D}$  with  $T$  joint observations of all the nodes at different time intervals, and 2) the observations at different time intervals are independent and identically distributed, i.e.,  $P(X_i^{(t)}, X_j^{(k)}) = P(X_i^{(t)})P(X_j^{(k)})$ , and  $P(X_i^{(t)}, X_j^{(t)}) = P(X_i^{(k)}, X_j^{(k)})$ ,  $\forall i, j$ , given that  $t \neq k$ .

The conditional probabilities for all the children nodes, namely  $\theta_{i,q,s} = P(X_i^{(t)} = x_i(q) | Y^{(t)} = y(s))$ , can be learned from the data with a maximum likelihood (ML) approach, i.e.,

$$\theta_{i,q,s}^* = \arg \max P(\mathcal{D} | \theta_{i,q,s}), \quad (18)$$

which in our case is equivalent to

$$\theta_{i,q,s}^* = \frac{\sum_{t=1}^T \mathbf{1}(X_i^{(t)} = x_i(q)) \mathbf{1}(Y^{(t)} = y(s))}{\sum_{t=1}^T \mathbf{1}(Y^{(t)} = y(s))}, \quad (19)$$

where  $\mathbf{1}(\cdot, \cdot)$  is the indicator function,  $\mathbf{1}(x, y) = 1$  if  $x = y$ , and  $\mathbf{1}(x, y) = 0$  otherwise.

The complexity of this ML approach for the estimation of the parameters in (19) is linear in  $T$ , the size of the dataset. We highlight that the BN learning should be executed only once at the beginning of the transmissions. As detailed in Sec. IV, the same BN can be used by each node to infer in constant time how much a given transmission is harmful to the cell where it takes place.

## C. BN data collection

The estimation of the BN starts with the collection of several instances of the parameters involved as inputs and outputs. We developed a full system level MATLAB network simulator, according to the system model described in Sec. III, and the protocol implementation introduced in Sec. IV. For each investigated scenario, we run the simulator for different random topologies, in which the nodes are randomly deployed over a square area of side  $L$ . We simulated 100 time slots for each topology, during which the protection mechanism employed by the BSs was not implemented, and the transmit power is randomly selected among the values in  $\Pi$ .

The rationale behind this approach is to consider all the parameters involved as multinomial random variables<sup>3</sup>, with a realization of each random variable at each time step  $k$ .

For every link involved in each simulation, a row of the dataset  $\mathcal{D}(\text{BN}_{\text{int}})$  is then filled with the chosen power level  $\pi_s$ , with the parameters in  $\mathcal{P}_C(U_S, k)$  and the corresponding capacity loss measured at the associated BS  $B^{(v)}$ .

We iteratively repeat the process of generating a new topology, run the simulation for 100 time slots and collect new rows in the dataset. The iterations end when  $\mathcal{D}(\text{BN}_{\text{int}})$  is filled with the minimum number of rows,  $n = 10^5$ .

## D. BN implementation

In a real network, the BN learning and data collection phases can be performed only once at the beginning of the network operations by collecting the parameters in  $\mathcal{P}_C(U_S, k)$ , defined in (12), at one or more nodes responsible for the learning phase. The resulting BN can then be used by each UE-LT to determine its mode/power selection. Differently from other learning mechanisms, whose reliability holds only for a given topology and hence for a limited amount of time, the BN learns a *stochastic* relationship among the network parameters. Therefore, it can still be used even when the topology changes, as long as the general network scenario (e.g., in terms of UE-LTs density) remains unaltered.

The BN learned at the beginning of the network operations is then used by each UE-LT, which exploits it for interference estimation, as detailed in Sec. IV-C.

## VI. RESULTS

In this section, we compare the performance of GEO-S, DPMS and AWA-S by using the same MATLAB system level simulator employed in the BN learning phase. For each set up of the parameters, we run 100 simulations over random topologies, each one lasting 100 time slots.

### A. Parameters setup

We set the values of our scenario parameters according to those commonly adopted in the literature [18], [29], thus resembling the relevant aspects of a real scenario. The simulated area is a square with side  $L = 5 \text{ km}$ . In this area, we set the BS intensity  $\lambda_V = 10 \text{ BSs/km}^2$ , the maximum UE transmit power  $P_M = 200 \text{ mW}$ , the path-loss exponent  $\alpha = 4$ , the SINR decoding threshold  $\phi = 1$ , and the noise power  $N_0 = -90 \text{ dBm}$ . The channel correlation coefficient  $\rho$  is set to 0.9; however, since the correlation level strongly affects the estimation accuracy, we plan to analyze the impact of different values of  $\rho$  in a future work. The epoch length is set to  $N_e = 10$  time slots, while the contention window for AWA-S spans over  $N_w = 4$  time slots. The target received power value is  $\rho = -70 \text{ dBm}$ , from which the maximum transmitting distance for GEO-S is  $d_R \simeq 210 \text{ m}$ . The maximum D2D link length is instead set to  $d_L \simeq 120 \text{ m}$ .

<sup>3</sup>If the variable is not discrete, we quantize it in a given number of values, depending on the variable distribution. The higher this number, the better the representation of the variable, but the more complicated the inference of the conditional dependences.

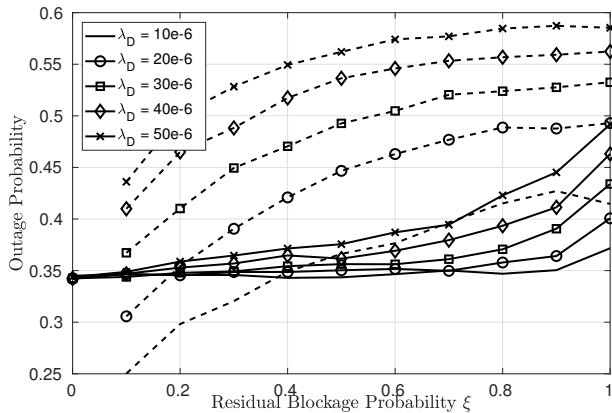


Fig. 2. SINR outage probability of AWA-S as a function of the residual blockage probability  $\xi$ . Solid lines are relative to D2B communications, while dashed lines refer to D2D communications.

### B. Performance metrics

In order to highlight different aspects of the techniques analyzed, we selected five performance metrics, described in the following. The performances are derived as a function of the bias factor,  $T_d$  (for GEO-S) or  $\xi$  (for AWA-S), which can be tuned to favor the D2B or D2D mode<sup>4</sup>.

**SINR outage probability.** This is the probability that the perceived SINR falls below the decoding threshold  $\phi$ , and can be derived from the SINR distribution. The SINR outage probability on the D2B links illustrates the impact of the additional interference from the D2D communications on the cellular users, while the SINR outage probability on the D2D links depicts the quality of the D2D transmissions.

**Fraction of UE-LTs in D2D mode.** In order to fully understand the network behaviors, it is pivotal to observe how often a UE-LT relies on direct D2D communications, as a function of the tunable parameter  $T_d$  (or  $\xi$ ).

**Spectral efficiency.** For a given source  $U$ , the spectral efficiency  $\mathcal{R}(U)$  of each user  $U$  is defined as per (7) and (8), averaged over all time slots. Notice that if the source  $U$  is not transmitting in a given time slot (e.g., because  $U$  is being forced to be silent, in AWA-S), its efficiency in that time slot is set to 0. We compute separately the average spectral efficiency of the UE-GTs and that of the UE-LTs, regardless of their effective transmission mode.

The spectral efficiency is a good indicator of the overall network performance. Differently from the SINR outage probability, which considers only active links, this metric also takes into account the advantages of offloading the traffic from the BS (thus reducing the users contending for the same channel).

**Network spectral efficiency.** This metric is used to evaluate the performance of the whole network. It is given by the sum of the average spectral efficiencies of a UE-GT and a UE-LT, each multiplied by the corresponding density ( $\lambda_V$  and  $\lambda_D$ , respectively), i.e.,

$$\mathcal{S} = \mathbb{E}_{U \in \mathcal{U}_g}[\mathcal{R}(U)]\lambda_V + \mathbb{E}_{U \in \mathcal{U}_\ell}[\mathcal{R}(U)]\lambda_D. \quad (20)$$

<sup>4</sup>Even if  $T_d$  can be any positive real number, we limit its value to the interval  $[0, 1]$ , since the best performance appears to be obtained for  $T_d \leq 1$ .

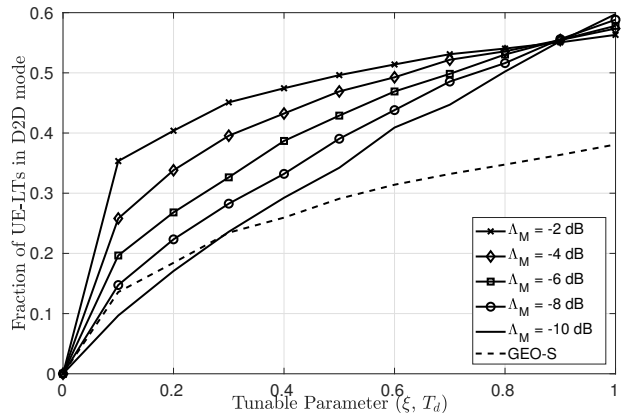


Fig. 3. Fraction of UE-LTs selecting D2D mode, as a function of  $T_d$  (for GEO-S), or  $\xi$  (for AWA-S). Here  $\lambda_D = 5\lambda_V$ .

This metric offers a global perspective on the network, measuring how efficiently the spectrum can be reused by D2B and D2D transmissions.

**Aggregate Throughput.** This metric is chosen to illustrate the overall network performance in terms of data delivery and reliability. A packet is delivered in a time slot if the transmission achieves a SINR greater than the decoding threshold  $\phi$ . The aggregate throughput is obtained as the total number of delivered packets divided by the simulation time. A packet delivered at the BS is also counted as a delivered packet, since we assume that the BS operates in full duplex over uplink and downlink channels, and that the bottleneck lies in the uplink.

### C. Link-level performance

In Fig. 2, we plot the observed SINR outage probability attained by our strategy AWA-S for both D2D and D2B communications when the maximum allowed relative capacity loss is  $\Lambda_M = 0.1$ , as a function of the biasing parameter  $\xi$  and for different values of the D2D pairs density  $\lambda_D$ . As expected, increasing the residual blockage probability  $\xi$  leads to a higher number of simultaneous D2D communications, thus raising the overall interference level. This in turn results in a higher outage probability for both D2D and D2B transmissions. Notice, however, that the outage probability grows faster for D2D communications. This is due to the presence of the blockage mechanism at the BSs, which promptly stops those communications causing a capacity loss higher than  $\Lambda_M$ . For low to medium densities of D2D pairs, this mechanism is effective in keeping the D2B outage probability at the BSs unaltered as long as  $\xi \leq 0.75$ , with only a minor increase for higher values. As the D2D pairs density grows, the blockage mechanism is less effective, since the overall interference is caused by a larger number of D2D transmitters, each causing a relatively low capacity loss. Nevertheless, by setting  $\xi \leq 0.3$ , the D2B outage remains almost unaltered even for  $\lambda_D = 5\lambda_V$ . For comparison, GEO-S has an outage probability for D2D links which ranges from 0.5 to 0.85 as  $\lambda_D$  grows. The outage probability for D2B links is close to the one achieved by AWA-S when  $\lambda_D = \lambda_V$ , but rapidly increases to 0.6 for  $\lambda_D = 5\lambda_V$ .

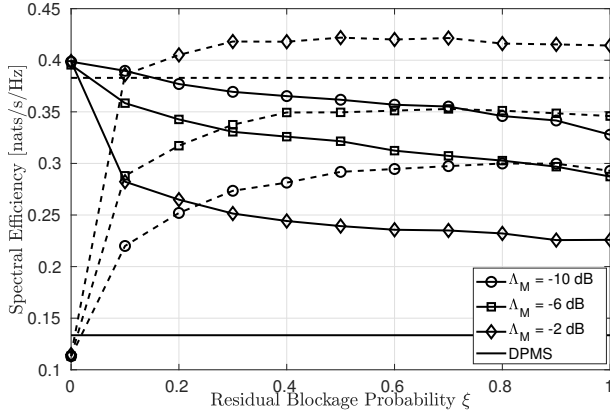


Fig. 4. Average user spectral efficiency, for  $\lambda_D = 5\lambda_V$ , as a function of  $\xi$ . Solid lines are for UE-GTs, while dashed lines are for UE-LTs.

In Fig. 3, we observe the fraction of UE-LTs that select D2D transmission mode, which can strongly affect the SINR outage probability. Here, we fix the D2D pair density  $\lambda_D = 5\lambda_V$ . For GEO-S, the fraction of D2D sources in D2D transmission mode is uniquely determined by the topology and, as expected, this value grows with  $T_d$ , regardless of the UE-LTs density. Nevertheless, even for  $T_d = 1$ , less than 40% of the UE-LTs select D2D mode.

For AWA-S, the fraction of UE-LTs selecting D2D mode also grows with  $\xi$ , since higher transmit power levels are allowed. The effect of  $\Lambda_M$  is also highlighted: the higher  $\Lambda_M$ , the faster the growth of the fraction of UE-LTs in D2D mode. This is reasonable, since a higher interference level is tolerated at the BS, and D2D transmissions become more convenient. Clearly, when  $\xi$  tends to 1, mode selection does not depend on  $\Lambda_M$  any more. In fact, condition (15) is always satisfied, and the D2D mode is chosen based only on condition (16), thus explaining why the curves tend to the same value when  $\xi = 1$ , between 55% and 60%.

#### D. Network-level performance

In this section we analyze the performance from a network-level perspective by observing the spectral efficiency of the whole network. In Fig. 4, we set  $\lambda_D = 5\lambda_V$  and we compute separately the spectral efficiency for UE-GTs and UE-LTs.

We compare AWA-S with the dynamic mode and power selection DPMS. We immediately observe that, for DPMS, the spectral efficiency of UE-LTs is much higher than that of UE-GTs. This is not surprising, since the mode and power selection for a UE-LT is based only on the performance of that user, and no countermeasures are taken to prevent excessively high interference levels at the BSs.

Things are much different with AWA-S, at least for low values of  $\xi$ . In this case, in fact, D2D transmissions are allowed only when they do not impair the communications of the UE-GTs. By tuning  $\xi$ , however, the spectral efficiency can be balanced between UE-LTs and UE-GTs. For  $\Lambda_M = -6$  dB a perfect balance is obtained when  $\xi = 0.3$ . We also observe that, for  $\Lambda_M = -2$  dB and high  $\xi$ , the spectral efficiency

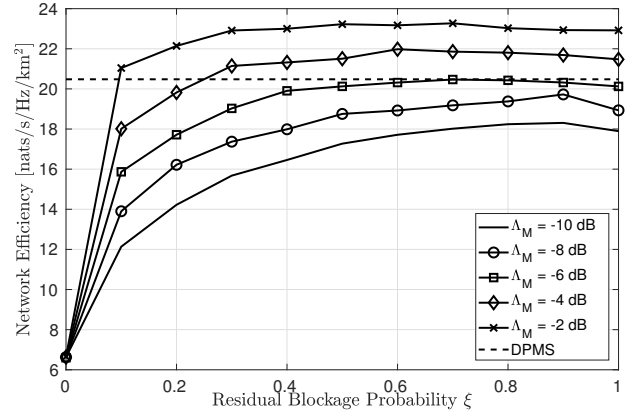


Fig. 5. Network spectral efficiency as a function of  $\xi$ . Here, the D2D pairs density is  $\lambda_D = 5\lambda_V$ .

for UE-LTs becomes 10% higher than that offered by DPMS, while still retaining an efficiency for UE-GTs 70% higher than the one attained by DPMS.

The overall gain can be investigated by looking at the network spectral efficiency, depicted in Fig. 5. Since  $\lambda_D$  is much higher than  $\lambda_V$ , improving the UE-LTs spectral efficiency by raising  $\xi$  has a global positive effect, even if the spectral efficiency of the UE-GTs is reduced. The network spectral efficiency grows with  $\xi$ , until it saturates, and is higher for low values of  $\Lambda_M$ . In fact, this makes D2D mode viable for more UE-LTs, thus improving the spatial reuse. AWA-S can outperform DPMS of up to 13% when  $\Lambda_M = -2$  dB. Notice, however, that a higher spectral efficiency does not always turn into a higher packet delivery rate, since it also implies a higher interference level, which increases the outage probability, as observed in Fig. 2.

In order to investigate the effective network performance, we now analyze the aggregate throughput. In Fig. 6 we illustrate the network throughput as a function of  $\xi$  in a scenario where  $\lambda_D = 3\lambda_V$ . We can observe some relevant behaviors. Firstly, it appears to be detrimental to increase  $\xi$  beyond a certain threshold, since it causes the overall throughput to be reduced, due to excessive interference. There is an optimal value of  $\xi$  which guarantees the highest performance. Secondly, this optimal value also depends on the maximum allowed capacity loss  $\Lambda_M$ . With the relatively low density  $\lambda_D = 3\lambda_V$ , the highest throughput is obtained with  $\Lambda_M = -2$  dB and  $\xi = 0.4$ . Thirdly, we compare the performance of AWA-S with that obtained by a centralized power and mode selection, which provides a local optimum and works as follows: in each cell, at the beginning of each epoch, the conditions of all the channels are collected, and the mode and power selection of all the users in the cell is performed by solving the optimization problem (6a) for the users within the cell via exhaustive search<sup>5</sup>. The computational complexity of

<sup>5</sup>This is not the global optimum, since the mode and power selection is done independently for each cell. Instead, it provides a realistic benchmark for comparison exploiting a large amount of information collected in a centralized fashion, while the amount of information required to compute the global optimum would make it impractical for this scenario.

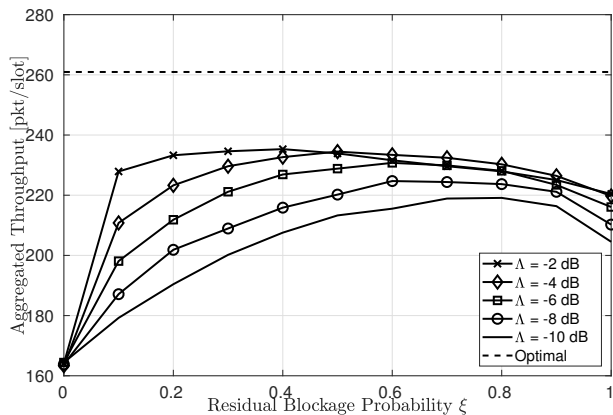


Fig. 6. Aggregated throughput, as a function of  $\xi$ . Here, the D2D pairs density is  $\lambda_D = 3\lambda_V$ .

this centralized approach is also quite high: with an average of 3 D2D pairs per cell, and 10 possible power levels, 1694 possible combinations are to be verified, a number which grows very fast in scenarios with higher D2D pairs densities. Conversely, in AWA-S, once the learning phase is completed, the computational burden at each D2D source grows linearly with the number of power levels, thus ensuring high scalability. Even if the centralized approach can exploit a far higher amount of information, AWA-S is still able to get a throughput which is only 10% lower.

Finally, in Fig. 7, we plot the aggregate throughput as a function of the UE-LT density, for all the considered strategies. For GEO-S and AWA-S we consider, for each density, the throughput obtained with the best selection of the corresponding parameter ( $T_d$  for GEO-S,  $\xi$  for AWA-S). GEO-S has the worst performance, due to the fact that it can only exploit static topology information. DPMS is the best choice, for low network densities, since the impact of D2D transmissions on the BSs remains limited. Nevertheless, as  $\lambda_D$  increases, the throughput of DPMS saturates. Our strategy AWA-S, conversely, can adaptively limit the growing interference caused by multiple simultaneous D2D communications. Even with a severe constraint ( $\Lambda_M = -10$  dB), AWA-S shows the same performance of DPMS for  $\lambda_D = 6\lambda_V$ . If  $\Lambda_M$  is increased to -4 dB, which is optimal for  $\lambda_S \geq 5\lambda_V$ , then the throughput is also increased, and AWA-S outperforms DPMS of up to 8% for  $\lambda_D = 7\lambda_V$ .

## VII. CONCLUSIONS

In this paper, we proposed a distributed approach that allows a mobile node with local traffic to acquire in real time local information by observing few channel and topology parameters. This information is utilized to perform a mode and power selection which takes into account also the capacity reduction caused at the BS. Our dynamic transmission strategy is hence able to adaptively switch between a D2D transmission, when the interference is limited, and a D2B transmission, otherwise. Power control is also performed targeting a balance between the quality of the D2D transmission and the impairment caused

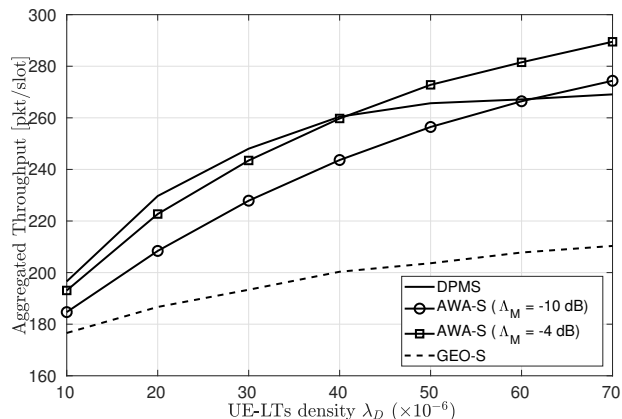


Fig. 7. Aggregated throughput, as a function of the UE-LTs density  $\lambda_D$ .

to the surrounding network. The comparison of our strategy with some state-of-the-art works in the same network scenario sheds light on the potential of the proposed learning mechanism and on the effectiveness of dynamic leveraging local information to perform a smart mode and power selection.

In a future work, we plan to extend the proposed technique keeping into consideration other constraints of the wireless network, like the energy consumption in each wireless node, and considering also multi-hop D2D communications.

## REFERENCES

- [1] 3GPP, "3rd generation partnership project; technical specification group sa; feasibility study for proximity services (ProSe) (release 12)," *TR 22.803 V1.0.0*, Aug. 2012.
- [2] L. Xingqin, J. G. Andrews, A. Ghosh, and R. Ratasuk, "An overview of 3GPP device-to-device proximity services," *IEEE Commun. Mag.*, vol. 52, no. 4, pp. 40–48, May 2014.
- [3] 3GPP, "3rd generation partnership project; technical specification group sa; study on architecture enhancements to support proximity services (ProSe) (release 12)," *TR 23.703 V0.4.1*, June 2013.
- [4] M. N. Tehrani, M. Uysal, and H. Yanikomeroglu, "Device-to-device communication in 5G cellular networks: challenges, solutions, and future directions," *IEEE Commun. Mag.*, vol. 52, no. 5, pp. 86–92, May 2014.
- [5] D. Feng, L. Lu, Y. Yuan-Wu, G. Y. Li, S. Li, and G. Feng, "Device-to-device communications in cellular networks," *IEEE Commun. Mag.*, vol. 52, no. 4, pp. 49–55, Apr. 2014.
- [6] L. Song, D. Niyato, Z. Han, and E. Hossain, *Wireless Device-to-Device Communications and Networks*. Cambridge University Press, 2014.
- [7] A. Zanella, N. Bui, A. Castellani, L. Vangelista, and M. Zorzi, "Internet of things for smart cities," *IEEE Internet of Things Journal*, vol. 1, no. 1, pp. 22–32, Feb. 2014.
- [8] L. Wei, R. Q. Hu, T. He, and Y. Qian, "Device-to-device (D2D) communications underlying MU-MIMO cellular networks," in *IEEE GLOBECOM*, Dec. 2013.
- [9] D. Feng, L. Lu, Y. Yuan-Wu, G. Y. Li, G. Feng, and S. Li, "Device-to-device communications underlying cellular networks," *IEEE Trans. Commun.*, vol. 61, no. 8, pp. 3541–3551, Aug. 2013.
- [10] Y. Li, C. Song, D. Jin, and S. Chen, "A dynamic graph optimization framework for multihop device-to-device communication underlying cellular networks," *IEEE Wireless Commun. Mag.*, vol. 21, no. 5, pp. 52–61, Oct. 2014.
- [11] B. Zhou, H. Hu, S.-Q. Huang, and H.-H. Chen, "Intracluster device-to-device relay algorithm with optimal resource utilization," *IEEE Trans. Veh. Technol.*, vol. 62, no. 5, pp. 2315–2326, June 2013.
- [12] M. G. Khoshkholgh, Y. Zhang, K.-C. Chen, K. G. Shin, and S. Gjessing, "Connectivity of cognitive device-to-device communications underlying cellular networks," *IEEE J. Select. Areas Commun.*, vol. 33, no. 1, pp. 81–89, Jan. 2015.

- [13] L. Wang, H. Tang, H. Wu, and G. L. Stüber, "Resource allocation for D2D communications underlay in rayleigh fading channels," *IEEE Trans. Veh. Technol.*, vol. 66, no. 2, pp. 1159–1170, Feb. 2017.
- [14] M. Sheng, Y. Li, X. Wang, J. Li, and Y. Shi, "Energy efficiency and delay tradeoff in device-to-device communications underlying cellular networks," *IEEE J. Select. Areas Commun.*, vol. 34, no. 1, pp. 92–106, Jan. 2016.
- [15] H. Tang, Z. Ding, S. J. B. Yoo, and J. Hämäläinen, "Outage constrained joint precoding for D2D underlay cellular networks," in *IEEE GLOBECOM*, Atlanta, GA, US, Dec. 2013, pp. 3540–3545.
- [16] F. Librino and G. Quer, "On the coexistence of D2D and cellular networks: an optimal distributed approach," in *Information Theory and Applications (ITA) Workshop*, Feb. 2017.
- [17] Y.-S. Liou, R.-H. Gau, and C.-J. Chang, "Group partition and dynamic rate adaptation for scalable capacity-region-aware device-to-device communications," *IEEE Trans. Wireless Commun.*, vol. 14, no. 2, pp. 921–934, Feb. 2015.
- [18] H. ElSawy, E. Hossain, and M. S. Alouini, "Analytical modeling of mode selection and power control for underlay D2D communication in cellular networks," *IEEE Trans. Commun.*, vol. 62, no. 11, pp. 4147–4161, Nov. 2014.
- [19] E. Naghipour and M. Rasti, "A distributed joint power control and mode selection scheme for D2D communication underlying LTE-A networks," in *IEEE Wireless Communication and Networking Conference*, Doha, Qatar, Apr. 2016.
- [20] D. Wu, Y. Cai, R. Quingyang Hu, and Y. Qian, "Dynamic distributed resource sharing for mobile D2D communications," *IEEE Trans. Wireless Commun.*, vol. 14, no. 10, pp. 5417–5429, Oct. 2015.
- [21] K. Akkarajitsakul, P. Phunchongharn, E. Hossain, and V. K. Bhargava, "Mode selection for energy-efficient D2D communications in LTE-advanced networks: a coalitional game approach," in *IEEE ICCS*, Singapore, Singapore, Nov. 2012.
- [22] S. Dominic and L. Jacob, "Distributed resource allocation for D2D communications underlying cellular networks in time-varying environment," *IEEE Commun. Lett.*, 2017, Early Access.
- [23] F. Librino, G. Quer, and M. Zorzi, "Network-aware retransmission strategy selection in ad hoc wireless networks," in *IEEE ICC*, Jun. 2013.
- [24] G. Quer, F. Librino, L. Canzian, L. Badia, and M. Zorzi, "Inter-network cooperation exploiting game theory and Bayesian networks," *IEEE Trans. Commun.*, vol. 61, no. 10, pp. 4310–4321, Oct. 2013.
- [25] F. Librino and G. Quer, "D2D Communications in the Uplink: a Context-Aware Approach with Punishment," in *IEEE GLOBECOM*, Dec. 2016.
- [26] D. Zordan, G. Quer, M. Zorzi, and M. Rossi, "Modeling and generation of space-time correlated signals for sensor network fields," in *IEEE GLOBECOM*, Dec. 2011.
- [27] D. Koller and N. Friedman, *Probabilistic Graphical Models: Principles and Techniques*. The MIT Press, 2009.
- [28] K. P. Murphy, *Machine Learning: A Probabilistic Perspective*. The MIT Press, 2012.
- [29] P. Joshi, D. Colombi, B. Thors, L. E. Larsson, and C. Törnevik, "Output power levels of 4G equipment and implications on realistic RF-EMF exposure assessments," *IEEE Access*, vol. 5, pp. 4545–4550, Mar. 2017.